

Impact of the LZ Experiment on DM Phenomenology and Naturalness in the MSSM

Li Dongwei¹, Meng Lei², and Zhou Haijing^{2*}

¹*Fundamentals Department , Henan Police College, Zhengzhou 450046, China*

²*School of Physics, Henan Normal University, Henan Xinxiang 453007, China*

Abstract

Taking the bino-dominated dark matter (DM) as an example, through approximate analytical formulas and numerical results, this paper analyzes impact of the LUX-ZEPLIN (LZ) Experiment on DM phenomenology and naturalness in Minimal Super-symmetric Standard Model(MSSM). It concluded that under the limitation of the latest LZ experiment, MSSM suffers unattractive fine-tunings. The reason is that the latest LZ experiment results improve μ bounds, e.g., for the cases of the Z - or h -mediated resonant annihilations to achieve the measured dark matter density, the LZ experiment require μ should be larger than about 500 GeV or TeV magnitude, which imply a tuning to predict the Z -boson mass and simultaneously worsen the naturalness of the Z - and h -mediated resonant annihilations to achieve the measured dark matter density.

arXiv:2312.01594v2 [hep-ph] 5 Dec 2023

*Email: zhouhaijing0622@163.com

1 Introduction

Supersymmetric models of particle physics are renowned for providing an elegant solution to the daunting gauge hierarchy problem. As the most economical supersymmetric extension model, the Minimal Supersymmetric Standard Model (MSSM) may provide a solid description of nature not only at the weak scale, but perhaps all the way up to energy scales associated with grand unification[1], which also receive indirect experimental support from the measured strengths of weak scale gauge couplings, the measured value of the top quark mass, and the discovery by ATLAS[2] and CMS[3] of a SM Higgs-like boson at 2012. However, such an audacious extrapolation has suffered a string of serious set-backs: so far, no signs of supersymmetric matter have emerged from LHC data or DM data, which has led some physicists to call into question whether or not weak scale SUSY really exists, or at least to concede that it suffers diversiform unattractive fine-tunings [4]. e.g., in 2017, the analysis of a global fit for the MSSM performed by considering various experimental constraints¹ showed that $\mu > 350\text{GeV}$ was favored at a 95% confidence level. Such a value of μ can induce a tuning of about 3% to predict the Z-boson mass.

In the MSSM, the Z boson mass is given by [8]

$$\frac{m_Z^2}{2} = \frac{m_{H_d}^2 + \Sigma_d^d - (m_{H_u}^2 + \Sigma_u^u) \tan^2 \beta}{\tan^2 \beta - 1} - \mu^2, \quad (1)$$

where $m_{H_u}^2$ and $m_{H_d}^2$ are soft SUSY breaking (not physical) Higgs mass terms, μ is the superpotential Higgsino mass term, $\tan \beta \equiv v_u/v_d$ is the ratio of Higgs field vevs and Σ_u^u and Σ_d^d include a variety of independent radiative corrections[9]. Since $(m_{H_d}^2 + \Sigma_d^d)$ term is suppressed by $\tan^2 \beta - 1$, for even moderate $\tan \beta$ values the expression Eq.(1) reduces approximately to

$$\frac{m_Z^2}{2} \simeq -(m_{H_u}^2 + \Sigma_u^u) - \mu^2. \quad (2)$$

In order to naturally achieve $m_Z \simeq 91.2\text{ GeV}$, $-m_{H_u}^2$, $-\mu^2$ and each contribution to $-\Sigma_u^u$ should all be nearby to $m_Z^2/2$ to within a factor of a few, which can be quantified using the electroweak fine-tuning parameter[10]

$$\Delta_{EW} \equiv \max_i |C_i| / (M_Z^2/2), \quad (3)$$

where $C_{H_u} = -m_{H_u}^2$, $C_\mu = -\mu^2$, and $C_{\Sigma_u^u} = \Sigma_u^u$. A low value of Δ_{EW} means less fine-tuning and $1/\Delta_{EW}$ is the % of fine-tuning., e.g. $\Delta_{EW} = 20$ corresponds to $\Delta_{EW}^{-1} = 5\%$ finetuning amongst terms contributing to $m_Z^2/2$. Researches in Ref. [11] showed that the higgsino mass μ should be larger than about 500 GeV for $M_1 < 0$ and 630 GeV for $M_1 > 100\text{ GeV}$ after considering the recent measurement of muon anomalous magnetic moment at Fermilab [12], the LUX-ZEPLIN (LZ) experiment just released its first results about the direct search for DM [13], and the rapid progress of the LHC search for supersymmetry[14, 15, 16]. These improved bounds imply a tuning of $\mathcal{O}(1\%)$ to predict the Z-boson mass.

¹These experimental constraints include those from the DM relic density, PandaX-II (2017) results for the SI cross section [5], PICO results for the SD cross section[6], and the searches for supersymmetric particles at the 13 TeV LHC with 36fb^{-1} data (especially the CMS analysis of the electroweakino production) [15].

In this paper, through approximate analytical formulas and numerical results, we analyze in detail the DM phenomenology and the associated unnaturalness in MSSM under the latest LZ experimental limits. The remainder of this paper is organized as follows. In section 2, we briefly introduce the neutralino sections of the MSSM, then demonstrate DM scattering cross-sections with nucleons and annihilation for bino-like $\tilde{\chi}_1^0$ through the approximate analytical formulas. In section 3, we provide a brief description of our scanning strategy and investigate at length predictions for surviving samples and the properties of bino-dominated DM scenarios to understand the associated unnaturalness. We reserve section 4 for our conclusions.

2 Dark Matter Section in the MSSM

In the MSSM, the neutralino mass matrix in the basis of $\Psi^0 = (-i\tilde{B}^0, -i\tilde{W}^0, \tilde{H}_d^0, \tilde{H}_u^0)$ is given by[17]:

$$M_{\text{neut}} = \begin{pmatrix} M_1 & 0 & -m_Z \cos \beta \sin \theta_w & m_Z \sin \beta \sin \theta_w \\ 0 & M_2 & m_Z \cos \beta \cos \theta_w & -m_Z \sin \beta \cos \theta_w \\ -m_Z \cos \beta \sin \theta_w & m_Z \cos \beta \cos \theta_w & 0 & -\mu \\ m_Z \sin \beta \sin \theta_w & -m_Z \sin \beta \cos \theta_w & -\mu & 0 \end{pmatrix}, \quad (4)$$

where M_1 , M_2 , and μ are the corresponding soft SUSY breaking mass parameters of the Bino, Wino, and Higgsinos, respectively. m_Z is the Z boson mass, θ_w is the Weinberg angle, and $\tan \beta = v_u/v_d$ is the ratio of the vacuum expectation values for the two Higgs doublets, and $v^2 = v_u^2 + v_d^2 = (246\text{GeV})^2$. Diagonalizing M_{neut} with a unitary matrix N of 4×4 yields the masses of the four neutralinos' physical states $\tilde{\chi}_i^0$ (ordered by mass):

$$N^* M_{\text{neut}} N^{-1} = \text{diag}\{m_{\chi_1^0}, m_{\chi_2^0}, m_{\chi_3^0}, m_{\chi_4^0}\}$$

with

$$\tilde{\chi}_i^0 = N_{i1}\tilde{B}^0 + N_{i2}\tilde{W}^0 + N_{i3}\tilde{H}_d^0 + N_{i4}\tilde{H}_u^0 \quad (i = 1, 2, 3, 4),$$

where m_{χ_i} are the roots to the following eigenequation

$$(x - M_1)(x - M_2)(x^2 - \mu^2) - m_Z^2(x - M_1 c_W^2 - M_2 s_W^2)(2\mu s_\beta c_\beta + x) = 0, \quad (5)$$

and the eigenvectors of m_{χ_i} is the column vector constituted by $N_{ij}(j = 1, 2, 3, 4)$ which given by

$$N_i = \frac{1}{\sqrt{C_i}} \begin{pmatrix} (\mu^2 - m_{\tilde{\chi}_i^0}^2)(M_2 - m_{\tilde{\chi}_i^0})s_W \\ -(\mu^2 - m_{\tilde{\chi}_i^0}^2)(M_1 - m_{\tilde{\chi}_i^0})c_W \\ (M_2 s_W^2 + M_1 c_W^2 - m_{\tilde{\chi}_i^0})(m_{\tilde{\chi}_i^0} c_\beta + \mu s_\beta)m_Z \\ -(M_2 s_W^2 + M_1 c_W^2 - m_{\tilde{\chi}_i^0})(m_{\tilde{\chi}_i^0} s_\beta + \mu c_\beta)m_Z \end{pmatrix}. \quad (6)$$

For the normalization factor C_i , its specific form is as follows

$$C_i = (\mu^2 - m_{\tilde{\chi}_i^0}^2)^2 (M_2 - m_{\tilde{\chi}_i^0})^2 s_W^2 + (\mu^2 - m_{\tilde{\chi}_i^0}^2)^2 (M_1 - m_{\tilde{\chi}_i^0})^2 c_W^2 \\ + (M_2 s_W^2 + M_1 c_W^2 - m_{\tilde{\chi}_i^0})^2 (\mu^2 + m_{\tilde{\chi}_i^0}^2 + 2\mu m_{\tilde{\chi}_i^0} s_\beta c_\beta) m_Z^2. \quad (7)$$

The diagonalizing matrix is then given by: $N = \{N_1, N_2, N_3, N_4\}$, where $i = 1, 2, 3, 4$ correspond to the bino, wino, higgsino-down and higgsino-up components respectively.

The lightest neutralino, $\tilde{\chi}_1^0$, acting as the DM candidate is the focus of this work. N_{11}^2 , N_{12}^2 and $N_{13}^2 + N_{14}^2$ respectively represent the bino, wino, and higgsino components in the physical state $\tilde{\chi}_1^0$, and satisfy $N_{11}^2 + N_{12}^2 + N_{13}^2 + N_{14}^2 = 1$. We call $\tilde{\chi}_1^0$ as bino-dominant DM (wino- or higgsino-) if $N_{11}^2 > 0.5$ ($N_{12}^2 > 0.5$ or $N_{13}^2 + N_{14}^2 > 0.5$). The couplings of DM to scalar Higgs states and the Z boson are included in the calculation of DM-nucleon cross sections and DM annihilation, which correspond to Lagrangian[18, 19]

$$\mathcal{L}_{MSSM} \ni C_{\tilde{\chi}_1^0 \tilde{\chi}_1^0 h} h \tilde{\chi}_1^0 \tilde{\chi}_1^0 + C_{\tilde{\chi}_1^0 \tilde{\chi}_1^0 H} H \tilde{\chi}_1^0 \tilde{\chi}_1^0 + C_{\tilde{\chi}_1^0 \tilde{\chi}_1^0 Z} Z_\mu \tilde{\chi}_1^0 \gamma^\mu \tilde{\chi}_1^0,$$

and the coefficients are given by

$$C_{\tilde{\chi}_1^0 \tilde{\chi}_1^0 h} \approx \frac{2m_Z^2 \mu}{v C_1} (\mu^2 - m_{\tilde{\chi}_1^0}^2) (M_2 s_W^2 + M_1 c_W^2 - m_{\tilde{\chi}_1^0})^2 \left(\frac{m_{\tilde{\chi}_1^0}}{\mu} + \sin 2\beta \right), \quad (8)$$

$$C_{\tilde{\chi}_1^0 \tilde{\chi}_1^0 H} \approx \frac{2m_Z^2 \mu}{v C_1} (\mu^2 - m_{\tilde{\chi}_1^0}^2) (M_2 s_W^2 + M_1 c_W^2 - m_{\tilde{\chi}_1^0})^2 \cos 2\beta, \quad (9)$$

$$C_{\tilde{\chi}_1^0 \tilde{\chi}_1^0 Z} \approx \frac{m_Z^3}{v C_1} (\mu^2 - m_{\tilde{\chi}_1^0}^2) (M_2 s_W^2 + M_1 c_W^2 - m_{\tilde{\chi}_1^0})^2 \cos 2\beta, \quad (10)$$

where h and H are two CP-even Higgs states predicted by the MSSM, respectively denoting the SM-like Higgs boson and non-SM doublet Higgs boson.

Serving as a weakly interacting massive particle (WIMP), $\tilde{\chi}_1^0$ might be detected by measuring their spin-independent (SI) and spin-dependent (SD) scattering cross-section after an elastic scattering of $\tilde{\chi}_1^0$ on a nucleus takes place. At the tree level, the contributes to the SD (SI) scattering cross-section in the heavy squark limit is dominated by the t-channel Z boson (CP-even Higgs bosons h_i) exchange diagram. Therefore, the scattering cross-sections take the following form [11, 20, 21]

$$\sigma_{\tilde{\chi}_1^0-N}^{SD} \approx C_N \times \left(\frac{C_{\tilde{\chi}_1^0 \tilde{\chi}_1^0 Z}}{0.01} \right)^2, \quad (11)$$

$$\begin{aligned} \sigma_{\tilde{\chi}_1^0-N}^{SI} &= \frac{m_N^2}{\pi v^2} \left(\frac{m_N m_{\tilde{\chi}_1^0}}{m_N + m_{\tilde{\chi}_1^0}} \right)^2 \left(\frac{1}{125 \text{GeV}} \right)^4 \times \\ &\quad \left\{ (F_u^N + F_d^N) C_{\tilde{\chi}_1^0 \tilde{\chi}_1^0 h} \left(\frac{125 \text{GeV}}{m_h} \right)^2 + \left(\frac{F_u^N}{\tan \beta} - F_d^N \tan \beta \right) C_{\tilde{\chi}_1^0 \tilde{\chi}_1^0 H} \left(\frac{125 \text{GeV}}{m_H} \right)^2 \right\}^2 \\ &\approx 6.4 \times 10^{-44} \text{cm}^2 \times \\ &\quad \left\{ (F_u^N + F_d^N) \frac{C_{\tilde{\chi}_1^0 \tilde{\chi}_1^0 h}}{0.1} \left(\frac{125 \text{GeV}}{m_h} \right)^2 + \left(\frac{F_u^N}{\tan \beta} - F_d^N \tan \beta \right) \frac{C_{\tilde{\chi}_1^0 \tilde{\chi}_1^0 H}}{0.1} \left(\frac{125 \text{GeV}}{m_H} \right)^2 \right\}^2, \quad (12) \end{aligned}$$

where $N=p, n$ respectively represent the proton and the neutron, and $C_p \simeq 2.9 \times 10^{-41} \text{cm}^2$ ($C_n \simeq 2.3 \times 10^{-41} \text{cm}^2$) [22, 23]. The form factors (at zero momentum transfer) are $F_d^{(N)} = f_d^{(N)} + f_s^{(N)} + \frac{2}{27} f_G^{(N)}$ and $F_u^{(N)} = f_u^{(N)} + \frac{4}{27} f_G^{(N)}$ with $f_q^{(N)} = m_N^{-1} \langle N | m_q q \bar{q} | N \rangle$ ($q = u, d, s$) representing the normalized light quark contribution to the nucleon mass, and $f_G^{(N)} = 1 - \sum_{q=u,d,s} f_q^{(N)}$ influencing other heavy quark mass fractions in nucleons [24, 25].

In the pure bino limit ($m_{\tilde{\chi}_1^0} \approx M_1$ and $N_{11}^2 \approx 1$), the above formulas can be approximated as

$$C_1 = (\mu^2 - m_{\tilde{\chi}_1^0}^2)^2 (m_{\tilde{\chi}_1^0} - M_2)^2 s_W^2, \quad (13)$$

$$C_{\tilde{\chi}_1^0 \tilde{\chi}_1^0 h} \approx \frac{2m_Z^2 \mu s_W^2}{v(\mu^2 - m_{\tilde{\chi}_1^0}^2)} \left(\frac{m_{\tilde{\chi}_1^0}}{\mu} + \sin 2\beta \right), \quad (14)$$

$$C_{\tilde{\chi}_1^0 \tilde{\chi}_1^0 H} \approx \frac{2m_Z^2 \mu s_W^2}{v(\mu^2 - m_{\tilde{\chi}_1^0}^2)} \cos 2\beta, \quad (15)$$

$$C_{\tilde{\chi}_1^0 \tilde{\chi}_1^0 Z} \approx \frac{m_Z^3 s_W^2}{v(\mu^2 - m_{\tilde{\chi}_1^0}^2)} \cos 2\beta. \quad (16)$$

Meanwhile, taking $F_d^{(N)} \simeq F_u^{(N)} \simeq 0.14$ and $\tan \beta \gg 1$, one can conclude that

$$\sigma_{\tilde{\chi}_1^0-n}^{SD} \approx 2.4 \times 10^{-40} \text{cm}^2 \times \frac{m_Z^2 v^2}{\mu^4} \times \left(\frac{1}{1 - m_{\tilde{\chi}_1^0}^2/\mu^2} \right)^2, \quad (17)$$

$$\begin{aligned} \sigma_{\tilde{\chi}_1^0-p}^{SI} &\approx 2.1 \times 10^{-45} \text{cm}^2 \times \frac{v^2}{\mu^2} \times \left(\frac{1}{1 - m_{\tilde{\chi}_1^0}^2/\mu^2} \right)^2 \\ &\times \left\{ \left(\frac{m_{\tilde{\chi}_1^0}}{\mu} + \sin 2\beta \right) \left(\frac{125 \text{GeV}}{m_h} \right)^2 + \frac{\tan \beta}{2} \left(\frac{125 \text{GeV}}{m_H} \right)^2 \right\}^2. \end{aligned} \quad (18)$$

The two analytic formulas suggest that σ^{SD} and σ^{SI} are suppressed by μ^4 and μ^2 , respectively. Moreover, if $(\frac{m_{\tilde{\chi}_1^0}}{\mu} + \sin 2\beta)$ and $\tan \beta$ have opposite signs, the contributions to σ^{SI} from the light (h) and heavy (H) Higgs exchange channels interfere destructively. And, σ^{SI} will vanish for $(\frac{m_{\tilde{\chi}_1^0}}{\mu} + \sin 2\beta) \left(\frac{1}{m_h} \right)^2 + \frac{\tan \beta}{2} \left(\frac{1}{m_H} \right)^2 \rightarrow 0$ which is known as the ‘‘generalized blind spot’’ [21, 26].

For DM produced via standard thermal freeze-out, the relic density at freeze-out temperature $T_F \equiv m_{\tilde{\chi}_1^0}/x_F$ (typically, $x_F \simeq 20$) are approximately as [21]

$$\Omega_{\tilde{\chi}_1^0} h^2 \sim 0.12 \times \frac{2.5 \times 10^{-26} \text{cm}^3/\text{s}}{\langle \sigma v \rangle_{x_F}}, \quad (19)$$

where $\langle \sigma v \rangle_{x_F}$ corresponds to the effective (thermally averaged) annihilation cross section. In order to match the observed DM relic density ($\Omega_{\text{DM}} h^2 \simeq 0.12$) [27], it is required that $\langle \sigma v \rangle_{x_F} \sim 2.5 \times 10^{-26} \text{cm}^3/\text{s}$.

In the MSSM, for $m_{\tilde{\chi}_1^0} < 1 \text{TeV}$, only the bino-dominated $\tilde{\chi}_1^0$ can predict the correct DM relic density, and the interactions of the higgsino- or wino-dominated $\tilde{\chi}_1^0$ with the Standard Model particles are relatively strong so that the predicted relic density is much smaller than the observed DM relic density [28]. In our scenario, taking the example of the bino-like $\tilde{\chi}_1^0$, it is to be discussed the fine-tunings introduced by DM sector in the MSSM under the current DM experimental limits. For bino-like $\tilde{\chi}_1^0$, the contributions to $\langle \sigma v \rangle_{x_F}$ from the following two channels

- The Z- or h-mediated resonant annihilation [29, 30], and the corresponding annihilation cross sections are respectively approximate to [31]

$$\langle\sigma v\rangle_{x_F}^{d\bar{d},Z} \simeq (2.5 \times 10^{-26} \frac{\text{cm}^3}{\text{s}}) \times \left[\left(\frac{0.46m_d}{1\text{GeV}} \right) \times \frac{C_{\tilde{\chi}_1^0\tilde{\chi}_1^0 Z}}{\left(1 - \frac{m_Z^2}{4m_{\tilde{\chi}_1^0}^2}\right)} \right]^2 \left(\frac{m_{\tilde{\chi}_1^0}}{46\text{GeV}} \right)^{-4}, \quad (20)$$

$$\langle\sigma v\rangle_{x_F}^{d\bar{d},h} \simeq (2.5 \times 10^{-26} \frac{\text{cm}^3}{\text{s}}) \times \left[\left(\frac{0.048m_d}{1\text{GeV}} \right) \times \frac{C_{\tilde{\chi}_1^0\tilde{\chi}_1^0 h}}{\left(1 - \frac{m_h^2}{4m_{\tilde{\chi}_1^0}^2}\right)} \right]^2 \left(\frac{m_{\tilde{\chi}_1^0}}{62\text{GeV}} \right)^{-2}. \quad (21)$$

Due to the hierarchy of the Yukawa couplings, the contribution to the thermal cross section from $(\chi\chi \rightarrow q\bar{q})$ annihilations will be dominated by the bottom quarks for lighter $m_{\tilde{\chi}_1^0}$. Here, m_d denotes down-type quark mass. As shown in the expression, the measured relic density requires a high degeneracy between $m_{Z(h)}$ and $2m_{\tilde{\chi}_1^0}$. We define degeneracy parameters $\delta_{Z(h)} = \left|1 - \frac{m_{Z(h)}^2}{4m_{\tilde{\chi}_1^0}^2}\right|$ to quantize the fine-tuning between $m_{Z(h)}$ and $2m_{\tilde{\chi}_1^0}$, e.g., $\delta_z = 10^{-3}$ implying 0.1% fine-tuning amongst m_Z and $2m_{\tilde{\chi}_1^0}$,

- The co-annihilation with sleptons, heavier neutralinos and/or charginos [29, 30, 32, 33, 34, 35, 36].

3 Numerical results and Theoretical analysis

We employed the MultiNest algorithm [37] with $n_{\text{live}} = 10000^2$ to comprehensively scan the following parameter space

$$\begin{aligned} 1 \leq \tan\beta \leq 60, \quad 0.1 \text{ TeV} \leq \mu \leq 1 \text{ TeV}, \quad 0.5 \text{ TeV} \leq M_A \leq 10 \text{ TeV}, \\ -1.0 \text{ TeV} \leq M_1 \leq 1.0 \text{ TeV}, \quad 0.1 \text{ TeV} \leq M_2 \leq 1.5 \text{ TeV}, \\ |A_t| = |A_b| \leq 5 \text{ TeV}, \quad 0.1 \text{ TeV} \leq M_{\tilde{\mu}_L}, M_{\tilde{\mu}_R} \leq 1 \text{ TeV}, \end{aligned}$$

where $\tan\beta$ was defined at the electroweak scale and the others were defined at the renormalization scale $Q = 1 \text{ TeV}$. In addition, other unimportant parameters were fixed at 3 TeV, which include the gluino mass M_3 , and the SUSY parameters of the first- and third-generation sleptons, and three generation squarks (except for the soft trilinear coefficients $A_t = A_b$ assumed to change freely). During the scan, we considered the experimental constraints including the consistency of h 's properties with the LHC Higgs data at the 95% confidence level (C.L.) [38], the collider searches for extra Higgs bosons [39], the $\pm 10\%$ around the central value of the DM relic density from the Planck-2018 data [27], the 90% C.L. upper bounds of the PandaX-4T experiment on the SI DM-nucleon scattering [40] and the XENON-1T experiment on the SD scattering [41], the 2σ bounds on the branching ratios of $B \rightarrow X_s\gamma$ and $B_s \rightarrow \mu^+\mu^-$ [42],

²The n_{live} parameter in the algorithm controlled the number of active points sampled in each iteration of the scan.

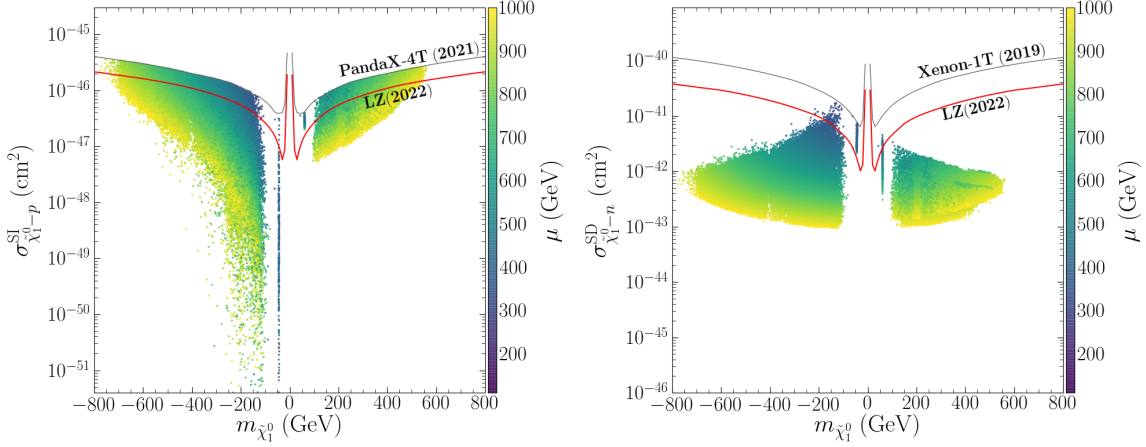


Figure 1: Projection of the obtained samples onto $m_{\tilde{\chi}_1^0} - \sigma_{\tilde{\chi}_1^0-p}^{SI}$ (left panel) and $m_{\tilde{\chi}_1^0} - \sigma_{\tilde{\chi}_1^0-n}^{SD}$ (right panel), respectively. The colors indicate the value of Higgsino mass μ .

and the vacuum stability of the scalar potential consisting of the Higgs fields and the last two generations of slepton fields [43, 44].

As presented in Fig.1, we respectively project the surviving samples on $m_{\tilde{\chi}_1^0} - \sigma_{\tilde{\chi}_1^0-p}^{SI}$ plane and $m_{\tilde{\chi}_1^0} - \sigma_{\tilde{\chi}_1^0-n}^{SD}$ plane, where the colors indicate the value of Higgsino mass μ . It can be clearly seen from Fig.1 that $\sigma_{\tilde{\chi}_1^0-n}^{SD}$ is only related to μ , and will be suppressed by a large μ , which is consistent with the analysis based on Eq.(17), namely, is proportional to $\frac{m_Z^2 v^2}{\mu^4}$. The current LZ experiment constraint on $\sigma_{\tilde{\chi}_1^0-n}^{SD}$ require μ is greater than 370 GeV. However, the distribution of $\sigma_{\tilde{\chi}_1^0-p}^{SI}$ values is relatively complex. Although large μ can suppress $\sigma_{\tilde{\chi}_1^0-p}^{SI}$, $\sigma_{\tilde{\chi}_1^0-p}^{SI}$ can also be small for small μ . Based on Eq.(18), $\sigma_{\tilde{\chi}_1^0-p}^{SI}$ should be related to a combination of M_1 , μ , $\tan \beta$, and m_H . To figure out what combination will make $\sigma_{\tilde{\chi}_1^0-p}^{SI}$ satisfy the latest experimental limit, as presented in Fig.2, we projected the surviving samples onto $m_{\tilde{\chi}_1^0} - (\frac{m_{\tilde{\chi}_1^0}}{\mu} + \sin 2\beta)$ plane and $m_{\tilde{\chi}_1^0} - M_2$ plane with colors indicating the value of Higgsino mass μ , and onto $(\frac{m_{\tilde{\chi}_1^0}}{\mu} + \sin 2\beta) - \frac{\tan \beta}{2} (\frac{125 \text{ GeV}}{m_H})^2$ plane and $(\frac{m_{\tilde{\chi}_1^0}}{\mu} + \sin 2\beta) - (\frac{v}{\mu})^2$ plane with colors indicating the value of $\sigma_{\tilde{\chi}_1^0-p}^{SI} \times 10^{48}$. From $(\frac{m_{\tilde{\chi}_1^0}}{\mu} + \sin 2\beta) - \frac{\tan \beta}{2} (\frac{125 \text{ GeV}}{m_H})^2$ plane, it is particularly easy to see that the contribution of Heavy Higgs (H) to the SI cross-section for the most samples is suppressed below 0.14 by m_H , and the contribution of the SM-like Higgs (h) plays an important role. Next, we divided the samples into the following three categories to discuss in detail.

1. Type-I samples: $m_{\tilde{\chi}_1^0} \approx -\frac{1}{2}m_Z$, $5 < \tan \beta < 58$, $337 \text{ GeV} < \mu < 462 \text{ GeV}$, $100 \text{ GeV} < M_2 < 1206 \text{ GeV}$. $\tilde{\chi}_1^0$ mainly annihilated to $d\bar{d}$ through exchange a resonant Z boson in the s-channel to get its measured relic density. According to Eq.(20), the corresponding annihilation cross section in this area is approximate to

$$\langle \sigma v \rangle_{x_F}^{d\bar{d},Z} \simeq (2.5 \times 10^{-26} \frac{\text{cm}^3}{\text{s}}) \left[\frac{2.2 \times 10^{-3} \times C_{\tilde{\chi}_1^0 \tilde{\chi}_1^0 Z}}{\delta_Z} \right]^2 \left(\frac{m_{\tilde{\chi}_1^0}}{46 \text{ GeV}} \right)^{-4}. \quad (22)$$

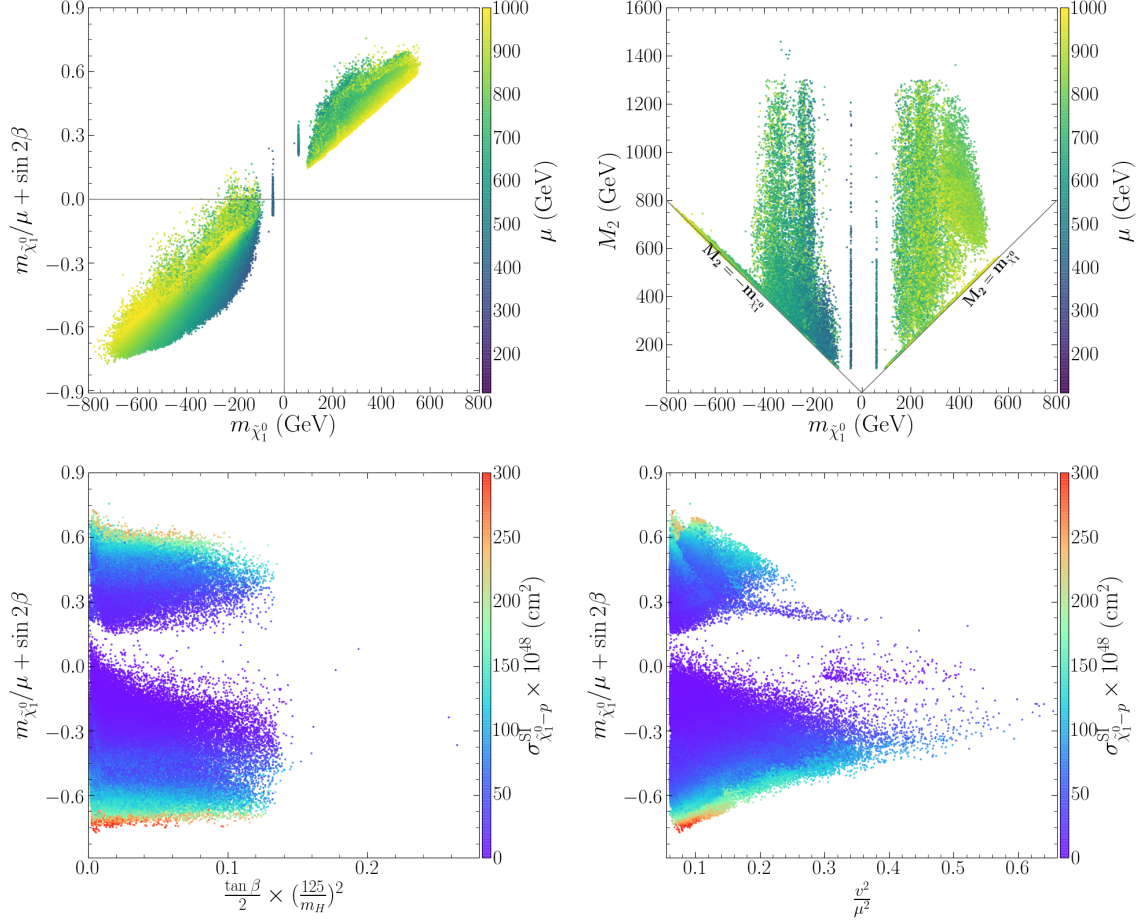


Figure 2: Projected the surviving samples onto $m_{\tilde{\chi}_1^0} - (\frac{m_{\tilde{\chi}_1^0}}{\mu} + \sin 2\beta)$ plane and $m_{\tilde{\chi}_1^0} - M_2$ plane with colors indicating the value of Higgsino mass μ , and onto $(\frac{m_{\tilde{\chi}_1^0}}{\mu} + \sin 2\beta) - \frac{\tan \beta}{2} (\frac{125 \text{ GeV}}{m_H})^2$ plane and $(\frac{m_{\tilde{\chi}_1^0}}{\mu} + \sin 2\beta) - (\frac{v}{\mu})^2$ plane with colors indicating the value of $\sigma_{\tilde{\chi}_1^0-p}^{SI} \times 10^{48}$.

In the case, from Figure 1, it is obviously seen that $\sigma_{\tilde{\chi}_1^0-p}^{SI}$ can satisfy direct detection constraints without large values of μ , but $\sigma_{\tilde{\chi}_1^0-n}^{SD}$ can not. As discussed above, $\sigma_{\tilde{\chi}_1^0-p}^{SI}$ is proportional to $(\frac{m_{\tilde{\chi}_1^0}}{\mu} + \sin 2\beta) + \frac{\tan \beta}{2} (\frac{125 \text{ GeV}}{m_H})^2$ in addition to being suppressed by μ^2 , and even vanishes under the limit of M_1 , μ , $\tan \beta$, and m_H being arranged. It can be seen from the top-left plane in Figure 2 that $|m_{\tilde{\chi}_1^0}/\mu + \sin 2\beta| < 0.1$ suppressing the SI cross section. However, $\sigma_{\tilde{\chi}_1^0-n}^{SD}$ is only proportional to $\frac{m_Z^2 v^2}{\mu^4}$. According to Eq.(17), the LZ direct detection constraints on SD cross section have required $\mu > 500 \text{ GeV}$ for these samples, corresponding to $\Delta_{EW}^{-1} = 1.7\%$. According to Eq.(16), $\mu = 500 \text{ GeV}$ corresponds to $C_{\tilde{\chi}_1^0 \tilde{\chi}_1^0 Z} = 3 \times 10^{-3}$ and $\delta_z = 6.6 \times 10^{-6}$, which implies a tuning of $\mathcal{O}(0.0001\%)$ to predict the right relic density. The larger μ is, the more severe this fine-tuning is, which is the main reason that μ cannot be very large in this case.

2. Type-II samples: $m_{\tilde{\chi}_1^0} \simeq \frac{1}{2} m_h$, $7 < \tan \beta < 33$, $406 \text{ GeV} < \mu < 776 \text{ GeV}$, $100 \text{ GeV} < M_2 <$

994GeV. $\tilde{\chi}_1^0$ mainly annihilated to $b\bar{b}$ through the s-channel exchange of a resonant SM-like Higgs boson h to get its measured relic density. According to Eq.(21), the corresponding annihilation cross section is approximate to

$$\langle\sigma v\rangle_{x_F}^{b\bar{b},h} \simeq (2.5 \times 10^{-26} \frac{\text{cm}^3}{\text{s}}) \left[\frac{0.2 \times C_{\tilde{\chi}_1^0 \tilde{\chi}_1^0 h}}{\delta_h} \right]^2 \left(\frac{m_{\tilde{\chi}_1^0}}{62\text{GeV}} \right)^2. \quad (23)$$

Compared with the Type-I samples, the μ value increases in the case. For the most samples, $\mu > 500\text{GeV}$ so that $\sigma_{\tilde{\chi}_1^0-n}^{SD}$ can satisfy direct detection constraints, but $\sigma_{\tilde{\chi}_1^0-p}^{SI}$ can not. From Figure 2, it can be seen that the range of $(m_{\tilde{\chi}_1^0}/\mu + \sin 2\beta)$ is (0.2,0.37), and the elevating effect of $(\frac{m_{\tilde{\chi}_1^0}}{\mu} + \sin 2\beta) + \frac{\tan\beta}{2}(\frac{125\text{GeV}}{m_H})^2$ on $\sigma_{\tilde{\chi}_1^0-p}^{SI}$ has an advantage over the suppressing effect of μ^2 . For $\tan\beta = 10(30)$, according to Eq.18, it is obtain that the direct detection constraints on SI cross section have raised μ to more than 1500GeV (1200GeV) corresponding to $\Delta_{EW}^{-1} = 0.2\%(0.3\%)$. According to Eq.(14), for $\mu = 1500\text{GeV}(1200\text{GeV})$, $C_{\tilde{\chi}_1^0 \tilde{\chi}_1^0 h} = 3(4) \times 10^{-3}$, in which the right relic density requires $\delta_h = 6(8) \times 10^{-4}$, namely, brings into a tuning of $\mathcal{O}(0.01\%)$.

3. Type-III samples: $m_{\tilde{\chi}_1^0} \in (-800, -100)\text{GeV} \cup (100, 550)\text{GeV}$, $5 < \tan\beta < 60$, $300\text{GeV} < \mu < 1000\text{GeV}$, $100\text{GeV} < M_2 < 1420\text{GeV}$, and $\tilde{\chi}_1^0$ mainly co-annihilated with sleptons or wino-dominated electroweakinos to achieve the measured density. As you can see from the top-left plane in figure 2, the cases with $-400\text{GeV} < m_{\tilde{\chi}_1^0} < -100\text{GeV}$ exist the "generalized blind spot" so that $\sigma_{\tilde{\chi}_1^0-p}^{SI}$ can be achieved to be small for small μ . However, the latest LZ experiment has required $\mu > 380\text{GeV}$; for the samples with $100\text{GeV} < m_{\tilde{\chi}_1^0} < 550\text{GeV}$, the contributions from h and H on $\sigma_{\tilde{\chi}_1^0-p}^{SI}$ reinforce each other so that $\sigma_{\tilde{\chi}_1^0-p}^{SI}$ is relatively large and the latest LZ experiment has raised μ to above 600 GeV corresponding to $\Delta_{EW}^{-1} = 1\%$. Moreover, this region will further shrink or even disappear with further improvement of sensitivity in future experiments, and the region with $-800\text{GeV} < m_{\tilde{\chi}_1^0} < -400\text{GeV}$ have a similar situation.

From the above analysis, it is clear that in the face of the latest dark matter experimental results, MSSM becomes very unnatural in order to simultaneously explain the dark matter scattering cross section and residual density. This situation will be further exacerbated if future DM DD experiments fail to detect the sign of the DM.

4 Conclusion

The LZ experiment just released its first results about the direct search for DM, where the sensitivities to spin-independent (SI) and spin-dependent (SD) cross sections of DM-nucleon scattering have reached about $6.0 \times 10^{-48} \text{cm}^2$ and $1.0 \times 10^{-42} \text{cm}^2$, respectively, for the DM mass around 30 GeV [13]. These unprecedented precision values strongly limit the DM coupling to the SM particles, which are determined by SUSY parameters. Faced with this strong experimental limitation, the DM phenomenology and the unnaturalness related to DM physics in MSSM is discussed in detail through by approximate analytical formulas. The study found that under

the limit of the latest dark matter experiment, the unnaturalness associated with DM in MSSM is embodied in large higgsino mass(μ) raised by the latest LZ experiment requirement, e.g., for the cases of the Z - or h -mediated resonant annihilations to achieve the measured dark matter density, the LZ experiment require μ should be larger than about 500 GeV or TeV magnitude. These improved bounds imply a tuning to predict the Z -boson mass and simultaneously worsen the naturalness of the Z - and h -mediated resonant annihilations to achieve the measured dark matter density.

Acknowledgments

We sincerely thank Prof. Junjie Cao for numerous helpful discussions and his great efforts to improve the manuscript.

References

- [1] S. P. Martin, In *Perspectives on supersymmetry II*, edited by G. L. Kane: 1-153 [hep-ph/9709356].
- [2] G. Aad *et al.* [ATLAS Collaboration], *Phys. Lett. B* **716** (2012) 1.
- [3] S. Chatrchyan *et al.* [CMS Collaboration], *Phys. Lett. B* **716** (2012) 30.
- [4] See *e.g.* M. Shifman, *Mod. Phys. Lett. A* **27** (2012) 1230043.
- [5] X. Cui *et al.* [PandaX-II], *Phys. Rev. Lett.* **119** (2017) no.18, 181302 doi:10.1103/PhysRevLett.119.181302 [arXiv:1708.06917 [astro-ph.CO]].
- [6] C. Amole *et al.* [PICO], *Phys. Rev. Lett.* **118** (2017) no.25, 251301 doi:10.1103/PhysRevLett.118.251301 [arXiv:1702.07666 [astro-ph.CO]].
- [7] A. M. Sirunyan *et al.* [CMS], *JHEP* **03** (2018), 160 doi:10.1007/JHEP03(2018)160 [arXiv:1801.03957 [hep-ex]].
- [8] H. Baer and X. Tata, *Weak Scale Supersymmetry: From Superfields to Scattering Events*, (Cambridge University Press, 2006).
- [9] H. Baer, V. Barger, P. Huang, A. Mustafayev and X. Tata, *Phys. Rev. Lett.* **109** (2012) 161802; H. Baer, V. Barger, P. Huang, D. Mickelson, A. Mustafayev and X. Tata, arXiv:1212.2655 [hep-ph].
- [10] H. Baer, V. Barger and M. Padeffke-Kirkland, *Phys. Rev. D* **88** (2013), 055026 doi:10.1103/PhysRevD.88.055026 [arXiv:1304.6732 [hep-ph]].
- [11] Y. He, L. Meng, Y. Yue and D. Zhang, [arXiv:2303.02360 [hep-ph]].
- [12] MUON G-2 collaboration, B. Abi *et al.*, *Phys. Rev. Lett.* **126** (2021) 141801.
- [13] LZ collaboration, J. Aalbers *et al.*, 2207.03764.

- [14] ATLAS collaboration, G. Aad et al., *Eur. Phys. J. C* **81** (2021) 1118.
- [15] CMS collaboration, A. M. Sirunyan et al., *JHEP* **03** (2018) 160.
- [16] CMS collaboration, A. M. Sirunyan et al., *JHEP* **03** (2018) 166
- [17] A. Pierce, N. R. Shah and K. Freese, [arXiv:1309.7351 [hep-ph]].
- [18] H. E. Haber and G. L. Kane. *Phys. Rept.* **117** (1985) 75.
- [19] J.F. Gunion and H.E. Haber. *Nucl. Phys. B* **272** (1986) 1[Nuclear Physics B 402.1-2(1993):569].
- [20] S. Baum, M. Carena, N. R. Shah, and C. E. M. Wagner, *JHEP* **01** (2022) 025.
- [21] S. Baum, M. Carena, T. Ou, D. Rocha, N. R. Shah and C. E. M. Wagner, *JHEP* **11** (2023), 037 doi:10.1007/JHEP11(2023)037 [arXiv:2303.01523 [hep-ph]].
- [22] M. Badziak, M. Olechowski and P. Szczerbiak, *JHEP* **1603**, 179 (2016) doi:10.1007/JHEP03(2016)179 [arXiv:1512.02472 [hep-ph]].
- [23] M. Badziak, M. Olechowski and P. Szczerbiak, *JHEP* **1707**, 050 (2017) doi:10.1007/JHEP07(2017)050 [arXiv:1705.00227 [hep-ph]].
- [24] M. Drees and M. M. Nojiri, *Phys. Rev. D* **48**, 3483 (1993) doi:10.1103/PhysRevD.48.3483 [hep-ph/9307208].
- [25] M. Drees and M. M. Nojiri, *Phys. Rev. D* **47**, 4226 (1993) doi:10.1103/PhysRevD.47.4226 [hep-ph/9210272].
- [26] P. Huang and C. E. M. Wagner, “Blind Spots for neutralino Dark Matter in the MSSM with an intermediate m_A ,” *Phys. Rev. D* **90**, 015018(2014).
- [27] **Planck** Collaboration, N. Aghanim *et al.*, “Planck 2018 results. VI. Cosmological parameters,” *Astron. Astrophys.* **641** (2020) A6 [Erratum: *Astron.Astrophys.* 652, C4 (2021)].
- [28] J. Cao, L. Meng, Y. Yue, H. Zhou and P. Zhu, *Phys. Rev. D* **101** (2020) no.7, 075003 doi:10.1103/PhysRevD.101.075003 [arXiv:1910.14317 [hep-ph]].
- [29] T. Han, Z. Liu, and A. Natarajan, “Dark matter and Higgs bosons in the MSSM, *JHEP* **11** (2013) 008.
- [30] M. E. Cabrera, J. A. Casas, A. Delgado, *et al.*, “Naturalness of MSSM dark matter, *JHEP* **08** (2016) 058.
- [31] S. Baum, M. Carena, N. R. Shah and C. E. M. Wagner, *JHEP* **04** (2018), 069 doi:10.1007/JHEP04(2018)069 [arXiv:1712.09873 [hep-ph]].
- [32] J. R. Ellis, T. Falk, and K. A. Olive, “Neutralino - Stau coannihilation and the cosmological upper limit on the mass of the lightest supersymmetric particle, *Phys. Lett. B* **444** (1998) 367–372
- [33] J. R. Ellis, T. Falk, K. A. Olive, and M. Srednicki, “Calculations of neutralino-stau coannihilation channels and the cosmologically relevant region of MSSM parameter space,” *Astropart. Phys.* **13** (2000) 181–213, [Erratum: *Astropart.Phys.* 15, 413–414 (2001)].

- [34] M. R. Buckley, D. Hooper, and J. Kumar, “Phenomenology of Dirac Neutralino Dark Matter, Phys. Rev. D **88** (2013) 063532,
- [35] M. J. Baker and A. Thamm, “Leptonic WIMP Coannihilation and the Current Dark Matter Search Strategy,” JHEP **10** (2018) 187,
- [36] T. T. Yanagida, W. Yin, and N. Yokozaki, “Bino-wino coannihilation as a prediction in the E_7 unification of families,” JHEP **12** (2019) 169,
- [37] F. Feroz, M. P. Hobson and M. Bridges, *MultiNest: an efficient and robust Bayesian inference tool for cosmology and particle physics*, Mon. Not. Roy. Astron. Soc. **398** (2009) 1601.
- [38] P. Bechtle, S. Heinemeyer, T. Klingl, T. Stefaniak, G. Weiglein and J. Wittbrodt, *HiggsSignals-2: Probing new physics with precision Higgs measurements in the LHC 13 TeV era*, Eur. Phys. J. C **81** (2021) 145.
- [39] P. Bechtle, D. Dercks, S. Heinemeyer, T. Klingl, T. Stefaniak, G. Weiglein et al., *HiggsBounds-5: Testing Higgs Sectors in the LHC 13 TeV Era*, Eur. Phys. J. C **80** (2020) 1211.
- [40] PANDAX-4T collaboration, Y. Meng et al., *Dark Matter Search Results from the PandaX-4T Commissioning Run*, Phys. Rev. Lett. **127** (2021) 261802.
- [41] XENON collaboration, E. Aprile et al., *Constraining the spin-dependent WIMP-nucleon cross sections with XENON1T*, Phys. Rev. Lett. **122** (2019) 141301.
- [42] PARTICLE DATA GROUP collaboration, M. Tanabashi, K. Hagiwara, Hikasa et al., Phys. Rev. D **98** (2018) 030001.
- [43] J. E. Camargo-Molina, B. O’Leary, W. Porod and F. Staub, *Vevacious: A Tool For Finding The Global Minima Of One-Loop Effective Potentials With Many Scalars*, Eur. Phys. J. C **73** (2013) 2588.
- [44] J. E. Camargo-Molina, B. Garbrecht, B. O’Leary, W. Porod and F. Staub, *Constraining the Natural MSSM through tunneling to color-breaking vacua at zero and non-zero temperature*, Phys. Lett. B **737** (2014) 156.